Heteroatom Chemistry
Volume 16, Number 5, 2005

Synthesis and Magnetic Properties of New Dinuclear Iron(II) Complexes of a Phenylene-Bridge Shiff Base Analogue Dinucleating Ligand

Birgit Weber and Eike Kaps

Department of Chemistry and Biochemistry, Ludwig Maximilian University Münich, Butenandtstr. 5-13 (Haus D), D-81377 München, Germany

Revised 3 February 2005

ABSTRACT: *The synthesis and magnetic behavior of four new dinuclear iron(II) complexes $Fe_2$2a-d × 4Py with the iron in an octahedral coordination sphere is presented in this paper. The complex* **c** *is a high-spin complex over the whole temperature range investigated, while the complexes* **a,b**, *and* **d** *perform a partial low-spin ⇔ high-spin spin transition. In case of $Fe_2$2b × 4Py, X-ray structure analysis of the HS/LS state was possible, showing that in one molecule both iron centers are either in the low-spin or sin the high-spin state.* © 2005 Wiley Periodicals, Inc. Heteroatom Chem 16:391–397, 2005; Published online in Wiley InterScience (www.interscience.wiley.com). DOI 10.1002/hc.20108

INTRODUCTION

Thermic-induced spin transitions without a change of the coordination number at the central atom are one of the most spectacular examples of molecular bistability. The change of properties during the phase transition is of technological interest, and several applications such as data storage devices can be imagined [1]. Octahedral iron(II) spin-crossover complexes are an important class of switchable molecules. The change of the spin state is accompanied by a change in the molecule size that is transmitted cooperatively through the crystal via intermolecular interactions. A high cooperativeness between the molecules leads to sharp spin transitions, sometimes even with hysteresis (memory effect) [1,2]. The mechanism of cooperativeness in spin transition compounds is well understood in terms of the model of internal pressure introduced by Spiering et al. [3]. However, the question of how to design such strongly cooperative complexes has still not been answered satisfactorily. A key factor is the effectiveness of the intermolecular contacts. The use of rigid linkers, which allow communication between the SCO centers by the formation of one-dimensional chains, two-dimensional layers, or three-dimensional networks, is one strategy for the purposeful synthesis of such compounds [2,4]. The simplest systems of spin-coupled polymers are dinuclear spin-crossover compounds with suitable bridging ligands. The investigation of such compounds provides fundamental information about the intramolecular magnetic interactions. So far only two families of dinuclear complexes have been investigated. One is the family of bpym-(2,2′-bipyrimidine)-bridged complexes investigated by Real et al. Partial or two-step spin crossover with spin-paired LS-LS, HS-LS, and HS-HS states have been realized [5] and recently

Dedicated to Professor Dr. Alfred Schmidpeter on the occasion of his 75th birthday.

Correspondence to: Birgit Weber; e-mail: bwmch@cup.uni-muenchen.de.

Contract grant sponsor: Deutsche Forschungsgemeinschaft.
Contract grant number: SPP 1137.
Contract grant sponsor: Fonds der Chemischen Industrie.

a example of a one-step spin-crossover complex of this family was reported [6]. The other family are bpypz-(3, 5-bis(pyridine-2-yl)pyrazolate)-bridged dinuclear iron complexes. Here the first abrupt spin-crossover without a two-step process was observed and the X-ray structure for both, the high-spin and the low-spin form was characterized [7].

In this work we want to introduce a new type of dinuclear iron(II) complexes where, instead of bridging ligands, a dinucleating chelate ligand is used to link the two iron centers together. In Scheme 1, the structure of the complex $Fe_2$2 and its mononucleating analogue Fe1 is given.

Iron(II) complexes of $H_2$1 with a broad variety of neutral axial ligands have been investigated in detail in the research group of E.-G. Jäger [8,9]. The octahedral diadducts of Fe1a with pyridine or imidazole perform a temperature-dependent low-spin (S = 0) ⇔ high-spin (S = 2) transition. In the case of Fe1a × 2py, the spin transition is gradual with a critical temperature of 220 K. The X-ray structure of both isomers could be determined [9]. The spin-crossover of Fe1a × 2Him is abrupt and shows a broad hysteresis around room temperature [9,10]. In the case of Fe1b, diadducts with pyridine and DMAP (4-*N*,*N*-dimethylaminopyridine) did also lead to spin crossover compounds. In both cases, the spin transition is abrupt and for the DMAP diadduct a small thermal hysteresis was observed. The X-ray structure of both isomers of Fe1b × 2py and the high-spin form of Fe1b × 2DMAP was determined [11]. Variation of the substituents a–d at the equatorial ligand leads to a defined influence on the electronic conditions and therefore the spin state of the metal center. This was observed for nitrosyl derivatives of iron complexes Fe1 and is also reflected in the magnetic properties of their pyridine and DMAP diadducts [11,12]. In this work, synthesis and characterization of the first dinuclear iron(II) complexes with pyridine as axial ligands will be presented. A copper and a vanadyl complex of this type were first prepared by Hendrickson et al. [13]. The copper complex shows weak antiferromagnetic interactions between the two copper centers, while for the vanadyl complex no interactions were observed. The six-coordinated iron(II) complex $Fe_2$2a × 4MeOH investigated in the research group of E.-G. Jäger shows meta-magnetic behavior [9].

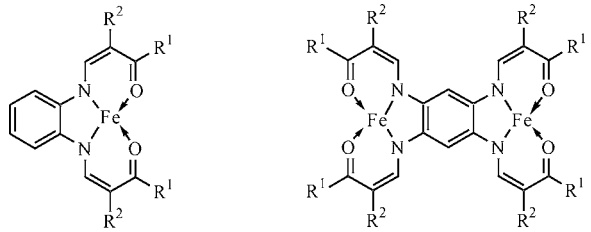

SCHEME 1 General structure of the iron(II) complexes discussed in this work.

EXPERIMENTAL SECTION

General Procedures and Instrumentation

If not described differently, all syntheses were carried out under argon using Schlenk tube techniques. All solvents were purified as described in the literature [14] and distilled under argon.

Magnetic measurements of pulverized samples were performed on a quantum-design-MPMSR-XL-SQUID-magnetometer in a temperature range from 5 to 295 K. All measurements were carried out at two field strengths (0.2 and 0.5 T). Diamagnetic corrections were made using values calculated with tabulated Pascal constants (as a rule, suitable values can be estimated as $\chi_{dia} \approx 0.5 \times 10^{-6} M_{complex}$). Thermogravimetric analyses were performed on Setaram TGA 92-24 instrument. Elementary analyses were performed on an Elementar Vario EL instrument.

Synthesis

The synthesis of the ligands $H_4$2a [9] and $H_4$2b [13] and iron(II) acetate [15] is described in the literature. The ligands $H_4$2c and $H_4$2d were prepared using the same procedure.

$Fe_2$2a × 4Py. Iron(II)acetate (0.46 g, 2.65 mmol) and $H_4$2a (0.71 g, 1.02 mmol) were dissolved in 50 mL pyridine and refluxed for 2 h. After cooling, the fine crystalline product was filtered off, washed with a little amount of methanol, and dried in vacuum. The mother solution was stored in the refrigerator for 1 week, to allow the slow crystalliztation of $Fe_2$2a × 4Py · 4Py. Yield: 0.55 g (60%).

Anal. Calcd for $C_{34}H_{38}N_4O_{12}Fe_2 \times 4C_5H_5N$: C, 57.77; H, 5.21; N, 9.98. Found: C, 54.50; H, 5.00; N, 8.45. IR (Nujol): ν(CO) = 1678 cm^{-1}. MS (DEI): base peak (M+): 805 *m/z* (100%); . DTG: up to 160°C: −13.2% = loss of two pyridine (theory: 15.8%); up to 250°C: −24.2% = loss of three pyridine (theory: 24.6%); at 320°C: decomposition.

$Fe_2$2b × 4Py. Iron(II)acetate (0.31 g, 1.78 mmol) and $H_4$2b (0.39 g, 0.685 mmol) were dissolved in 50 mL pyridine and refluxed for 2 h. After cooling to room temperature the solution was stored in the freezer for 2 months. The crystalline product was filtered off and dried in vacuum. Yield: 0.48 g (72%).

Anal. Calcd for $C_{30}H_{30}N_4O_8Fe_2 \times 4C_5H_5N$: C, 59.89; H, 5.03; N, 11.18. Found: C, 60.23; H, 5.20; N, 11.49. MS (FAB+): base peak(M+): 686 *m/z* (6%).

$Fe_2$2b × 4Py · Py. Iron(II)acetate (0.54 g, 3.105 mmol) and $H_4$2b (0.719 g, 1.242 mmol) were dissolved in 30 mL pyridine and refluxed for 2 h. After cooling to room temperature the solution was stored in the refrigerator for 2 days. The crystalline precipitate was filtered off and dried in vacuum. Yield: 0.55 g (38%). Some of those crystals were left in the mother solution and used for X-ray structure analysis giving $Fe_2$2b × 4Py·7Py.

Anal. Calcd for $C_{30}H_{30}N_4O_8Fe_2 \times 5C_5H_5N$: C, 61.07; H, 5.12; N, 11.65. Found: C, 61.73; H, 5.28; N, 11.98. IR (Nujol): ν(CO) = 1634 cm^{-1}. MS (FAB+): base peak (M+): 686 *m/z* (6%). DTG: up to 90°C: −6.9% = loss of one pyridine (theory: 7.3%); at 370°C: decomposition.

$Fe_2$2c × 4Py · Py. Iron(II)acetate (0.47 g, 2.7 mmol) and $H_4$2c (0.85 g, 1.03 mmol) were dissolved in 50 mL pyridine and refluxed for 1 h. After cooling, the fine crystalline product was filtered off, washed with a little amount of pyridine, and dried in vacuum. The mother solution was stored in the freezer overnight to produce a fine crystalline precipitate of Fe1c × 4Py · Py. Yield: 0.86 g (67%).

Anal. Calcd for $C_{38}H_{46}N_4O_{16}Fe_2 \times 5C_5H_5N$: C, 56.93; H, 5.32; N, 9.64. Found: C, 56.88; H, 5.43; N, 9.45. IR (Nujol): ν(CO) = 1693 cm^{-1}. MS (FAB+): base peak (M+): 926 *m/z* (100%). DTG: up to 110°C: −16.3% = loss of three pyridine (theory: 18.11%); up to 190°C: −26.1% = loss of five pyridine (theory: 30.1%); at 350°C: decomposition.

$Fe_2$2d × 4Py. Iron(II)acetate (0.24 g, 1.38 mmol) and $H_4$2d (0.35 g, 0.55 mmol) were dissolved in 40 mL pyridine and refluxed for 2 h. After cooling, the precipitate was filtered off, washed with a little amount of pyridine and dried in vacuum. Yield: 0.34 g (59%).

Anal. Calcd for $C_{30}H_{26}N_8O_8Fe_2 \times 4C_5H_5N$: C, 56.94; H, 4.40; N, 15.94. Found: C, 56.73; H, 4.40; N,15.60. MS (FAB+): Basis peak: 738 *m/z* (M+, 8.5%). DTG: up to 170°C: −35.9% = loss of four pyridine (theory: 30.0%); at 350°C: decomposition.

Crystal Structure Analysis

The intensity data for the compound $Fe_2$2b × 4Py · 7Py were collected on a Nonius KappaCCD diffractometer using graphite-monochromated Mo K_α radiation at 200 K and 125 K. The structures were solved by direct methods (SHELXS [16]) and refined by full-matrix least-square techniques against F_0^2 (SHELXL-97 [17]). The hydrogen atoms were included at calculated positions with fixed thermal parameters. All non-hydrogen atoms were refined anisotropically for the structure determined at 200 K. For the structure determined at 125 K, it was not possible to refine all non-hydrogen atoms anisotropically due to the large size of the structure.

The intensity data for the compound $Fe_2$2a × 4Py · 4Py were collected on a Stoe IPDS diffractometer using graphite-monochromated Mo K_α radiation. The structure was solved by direct methods (Sir 97 [18]) and refined by full-matrix least-square techniques against F_0^2 (SHELXL-97 [17]). The hydrogen atoms were included at calculated positions with fixed thermal parameters. All non-hydrogen atoms were refined anisotropically.

ORTEP-III was used for structure representation [19].

Crystal Data for $Fe_2$2a × 4Py · 4Py [20]. $C_{74}H_{78}N_{12}O_{12}Fe_2$, $M_r = 1439.172$ g mol^{-1}, triclinic, space group P-1, $a = 9.291(5), b = 14.173(5), c = 15.529(5)$ Å, $\alpha = 67.672(5)°$, $\beta = 76.561(5)°$, $\gamma = 72.914(5)°$, $V = 1791.1(13)$ Å^3, $T = 200(2)$ K, $Z = 1$, $\rho_{calcd.} = 1.332$ g cm^{-3}, μ(Mo K_α) = 0.71073Å, $F(000) = 752$, 15,561 reflections in h(−12/12), k(−18/18), l(−20/20), measured in the range $2.41° \le \Theta \le 28.02°$, 7951 independent reflections, $R_{int} = 0.039$, 5635 reflections with $F_0 > 4\sigma(F_0)$, 456 parameters, 0 restraints, $R1_{obs} = 0.043$, $R1_{all} = 0.067$, $wR^2 = 0.113$, GOOF = 0.931.

Crystal Data for $Fe_2$2b × 4Py · 7Py [20]. $C_{85}H_{85}N_{15}O_8Fe_2$, $M_r = 1556.372$ g mol^{-1}, triclinic, space group P-1, $a = 12.6120(3)$, $b = 13.1600(4)$, $c = 13.9320(4)$ Å, $\alpha = 75.1250(9)°$, $\beta = 63.9660(11)°$, $\gamma = 78.3330(13)°$, $V = 1997.39(10)$ Å^3, $T = 200(2)$ K, $Z = 1$, $\rho_{calcd.} = 1.295$ g cm^{-3}, μ (Mo K_α) = 0.71073Å, $F(000) = 816$, 19,157 reflections in h(−16/16), k(−17/16), l(−18/18), measured in the range $3.22° \le \Theta \le 27.46°$, 8970 independent reflections, $R_{int} = 0.077$, 4822 reflections with $F_0 > 4\sigma(F_0)$, 539 parameters, 0 restraints, $R1_{obs} = 0.081$, $R1_{all} = 0.156$, $wR^2 = 0.265$, GOOF = 1.014.

Crystal Data for $Fe_2$2b × 4Py · 7Py [20]. $C_{85}H_{85}N_{15}O_8Fe_2$, $M_r = 1556.372$ g mol^{-1}, triclinic, space

group $P\text{-}1$, $a = 18.6117(4)$, $b = 19.7495(5)$, $c = 22.0359(6)$ Å, $\alpha = 103.7747(10)^\circ$, $\beta = 96.0775(10)^\circ$, $\gamma = 92.5408(8)^\circ$, $V = 7802.3(3)$ Å^3, $T = 125(2)$ K, $Z = 4$, $\rho_{\text{calcd.}} = 1.325$ g cm^{-3}, $\mu(\text{Mo } K_\alpha) = 0.71073$ Å, $F(000) = 3264$, 478,644 reflections in $h(-24/24)$, $k(-24/25)$, $l(-28/28)$, measured in the range $3.18^\circ \leq \Theta \leq 27.53^\circ$, 35,442 independent reflections, $R_{\text{int}} = 0.156$, 15451 reflections with $F_0 > 4\sigma(F_0)$, 1488 parameters, 0 restraints, $R1_{\text{obs}} = 0.096$, $R1_{\text{all}} = 0.234$, $wR^2 = 0.261$, GOOF = 1.017.

RESULTS AND DISCUSSION

Synthesis and General Characterization

Replacing orthophenylenediamine used for the synthesis of the mononucleating Jäger ligands $H_2$1a–d with 1,2,4,5-tetraaminobenzol leads to the formation of phenylene-bridge dinucleating ligands $H_4$2a–d. Conversion of the ligands with iron(II) acetate in the presence of pyridine gives dinuclear iron(II) complexes with pyridine as the axial ligand. In order to ensure the formation of octahedral complexes is best to use the axial ligand as solvent. Methanol/pyridine mixtures, used for the synthesis of the octahedral mononuclear complexes, lead to the formation of penta-coordinated species or mixtures of the two.

In most cases the complexes crystallize with additional solvent in the crystal. The exact amount is difficult to determine because it is volatile, and elementary analysis in combination with thermogravimetric analysis generally yields a lower percentage compared with results from X-ray structure analysis. This is due to the fact that the crystals for X-ray structure analysis were stored in their mother solution, before measuring them. As soon as the complexes are dried in vacuum, some of the additional pyridine in the crystal evaporates and the crystals crumble. These dry powders were used for the magnetic measurement and all the other analysis. In order to differentiate between the pyridine in the crystal and the pyridine coordinated to the iron, the complexes will be abbreviated as FeX × APy · BPy with A being the number of pyridine molecules coordinated to the iron and B being the number of additional pyridine in the crystal.

X-ray Structure Analysis

Crystals suitable for X-ray structure analysis were obtained for $Fe_2$2a × 4Py · 4Py and $Fe_2$2b × 4Py · 7Py. In the case of $Fe_2$2b × 4Py · 7Py, it was possible to determine the structure before and after a partial spin transition. Selected bond lengths and angles within the first coordination sphere are given in Table 1. For the purpose of comparison, the results for the pyridine diadducts of the mononuclear complexes are included. In Fig. 1 an ORTEP drawing of the molecule structure of $Fe_2$2a × 4Py · 4Py is given.

At 200 K both complexes are in a $S_1 = 2$, $S_2 = 2$ state. The iron has an approximately octahedral coordination sphere and is located in the plane of the equatorial ligand. The average Fe-N/O distances of 2.09 Å (Fe-N_{eq}), 2.01 Å (Fe-O_{eq}), and 2.27 Å (Fe-N_{ax}) are comparable with those of the mononuclear complexes in their high-spin state. That also applies to the O–Fe–O angle (≈110°) that is known to be a sensible tool for detecting the spin state in SCO complexes of the Jäger ligand type [9,11]. Upon cooling, the cell volume of $Fe_2$2b × 4Py·7Py quadruplicates and significant changes in the cell parameters can be observed. Instead of one formula unit per cell, four are found, of which two are crystallographically independent. In Fig. 2 the results are displayed.

Comparison of the bond distances and angles with those obtained at 200 K shows that in one molecule both irons are still in the high-spin state (Fe3 ∠ O–Fe–O 110.8°; Fe4 ∠ O–Fe–O 112.2°), while in the other molecule both iron centers are in the low-spin state (Fe1 ∠ O–Fe–O 89.8°; Fe2 ∠ O–Fe–O 90.2°). Obviously, the complex performs a spin transition until half of the molecules are in their low-spin state. This might be due to a preferred 1:1 ordering of

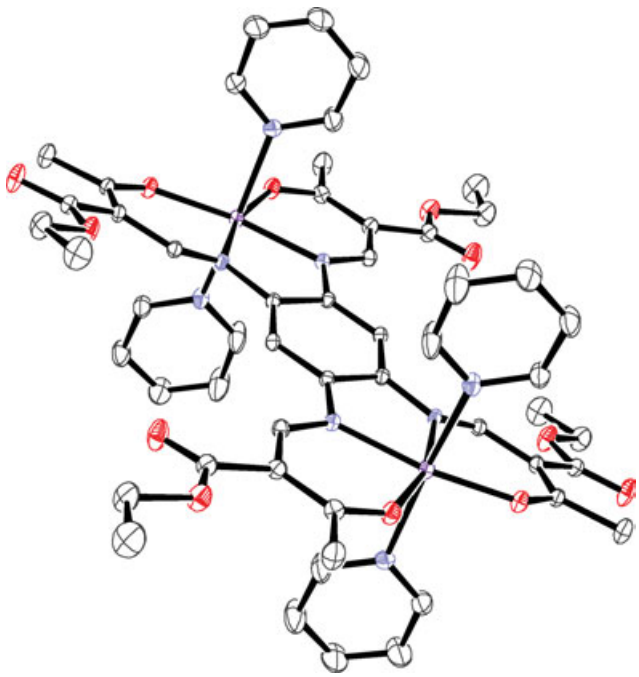

FIGURE 1 ORTEP drawing of the complex $Fe_2$2a × 4Py · 4Py at 200 K. The protons and additional pyridine in the crystal are omitted for clarity.

TABLE 1 Selected Bond Lengths and Angles within the First Coordination Sphere of Mono- and Dinuclear Iron(II) Complexes with Pyridine as Axial Ligand

Complex	*S*	*Fe–N_{eq}*	*Fe–O_{eq}*	*Fe–L_{ax}*	*∠O1–Fe–O2*	*∠L1, L2*[d]
$Fe_2$2a × 4Py · 4Py (200 K)	2; 2	2.0939 (18) 2.0975 (17)	2.0130 (17) 2.0144 (15)	2.264 (2) 2.307 (2)	110.22 (6)	3.9
$Fe_2$2b × 4Py · 7Py (200 K)	2; 2	2.077 (3) 2.079 (3)	2.006 (3) 2.017 (3)	2.231 (3) 2.289 (4)	109.0 (1)	36.7
$Fe_2$2b × 4Py · 7Py (125 K) Fe1	0	1.899 (4) 1.903 (4)	1.936 (4) 1.939 (4)	1.998 (5) 2.016 (5)	89.8 (2)	85.0
$Fe_2$2b × 4Py · 7Py (125 K) Fe2	0	1.895 (4) 1.895 (4)	1.948 (4) 1.950 (4)	2.005 (5) 2.007 (5)	90.2 (2)	82.3
$Fe_2$2b × 4Py · 7Py (125 K) Fe3	2	2.087 (4) 2.101 (4)	2.013 (4) 2.036 (4)	2.228 (5) 2.284 (5)	110.8 (2)	58.3
$Fe_2$2b × 4Py · 7Py (125 K) Fe4	2	2.092 (4) 2.099 (4)	2.020 (4) 2.034 (4)	2.208 (5) 2.290 (5)	112.2 (2)	79.4
Fe1a × 2Py[a]	2	2.062 (4) 2.053 (4)	2.017 (4) 1.990 (3)	2.256 (5) 2.195 (4)	106.3 (1)	80.1
Fe1a × 2Py[a]	0	1.923 (3) 1.918 (2)	1.962 (2) 1.955 (2)	2.023 (3) 2.025 (3)	92.4 (1)	78.9
Fe1b × 2Py[b]	2	2.0605 (15) 2.0737 (14)	1.9917 (13) 2.0092 (12)	2.2264 (17) 2.2687 (17)	106.99 (5)	16.70
Fe1b × 2Py[b]	0	1.8935 (14) 1.9060 (14)	1.9299 (12) 1.9476 (12)	2.0072 (16) 2.0247 (15)	89.98 (5)	15.40
Fe1c × 2Py[b]	2	2.109 (2) 2.102 (2)	2.0455 (14) 2.0481 (14)	2.239 (2) 2.262 (2)	112.04 (6)	43.4
Fe1d × 2Py · Py[c]	2	2.100 2.140	2.084 2.049	2.250 2.246	108.0	53.9

[a]cf. [9].
[b]cf. [11].
[c]cf. [21].
[d]Angle between the planes of the axial ligands.

high-spin and low-spin molecules in the crystal that was already found for some mononuclear complexes [1].

Magnetic Properties

Measurements of the magnetic susceptibilities were performed in the temperature range from 5 to 295 K for all complexes. The measurements were carried out at two field strengths. The effective magnetic moment μ_{eff} plotted against temperature is given in Fig. 3 for $Fe_2$2c × 4Py · Py and $Fe_2$2d × 4Py and in Fig. 4 for $Fe_2$2a × 4Py, $Fe_2$2b × 4Py, and $Fe_2$2b × 4Py · Py. As the measurements were performed on dry, pulverized samples, the molecular weight used for the interpretation of the data is the molecular

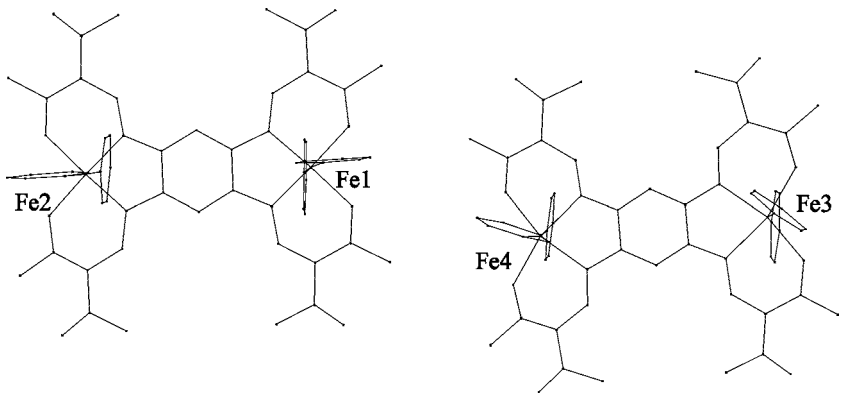

FIGURE 2 Asymmetric unit of $Fe_2$2b×4Py · 7Py at 125 K. The protons and additional pyridine in the crystal are omitted for clarity.

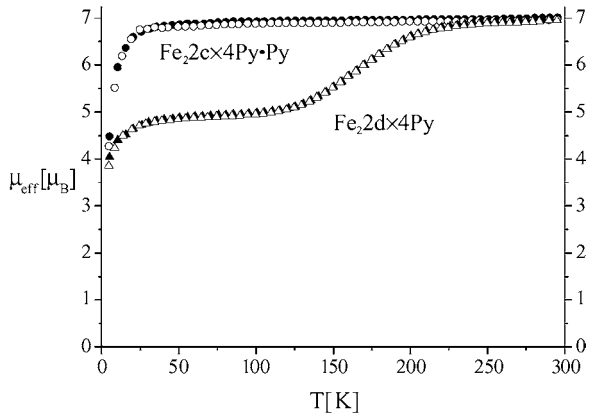

FIGURE 3 Effective magnetic moment versus temperature for the dinuclear octahedral iron(II) complexes $Fe_2$2c × 4Py·Py (circles) and $Fe_2$2d × 4Py (triangles), measured at 2000 G and 5000 G.

weight obtained by elementary analysis and the amount of additional pyridine in the crystals diverges significantly from those obtained by the X-ray structure analysis.

At room temperature, all complexes except $Fe_2$2b × 4Py·Py exhibit an effective magnetic moment at around 7 μ_B typical for two high-spin iron(II) centers according to $\mu_{eff} = 2\sqrt{S_1(S_1+1) + S_2(S_2+1)}$. For $Fe_2$2c × 4Py·Py the moment is constant down to 25 K, where a small decrease can be observed. Assuming the formula given in [5a] for the magnetic interactions in a $S_1 = 2$ and $S_2 = 2$ spin system with $H = -JS_2 \cdot S_2$, a weak antiferromagnetic interaction can be estimated to be $J = -1.08$ cm^{-1} ($g = 1.96$) by fitting the observed data given in Fig. 3. This coupling is significantly smaller than those observed for

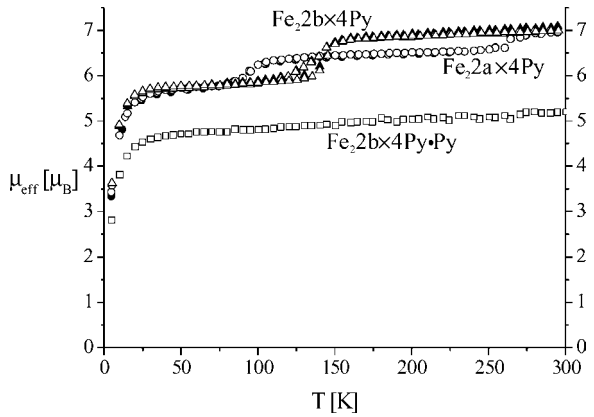

FIGURE 4 Effective magnetic moment versus temperature for the dinuclear octahedral iron(II) complexes $Fe_2$2a × 4Py (circles), $Fe_2$2b × 4Py (triangles), and $Fe_2$2b × 4Py · Py (squares), measured at 2000 G and 5000 G.

bpym- and bpypz-bridged complexes (J = ca. −4 to −3.5 cm^{-1}).

In the case of $Fe_2$2d × 4Py, the magnetic moment decreases below 225 K and reaches a second plateau at 100 K with $\mu_{eff} = 4.95$ μ_B typical for a $S_1 = 0$ and $S_2 = 2$ system. The spin transition is gradual. No additional data are available to decide how the two different iron centers are spread in the molecule or the crystal.

The spin transition behavior of the complexes $Fe_2$2a and $Fe_2$2b depends significantly on the amount of solvent molecules in the crystal. In Fig. 4 the temperature dependence of the magnetic moment of $Fe_2$2b × 4Py with no and one additional pyridine per complex in the crystal is compared. With no additional pyridine in the crystal, a stepwise spin transition with a small hysteresis can be observed. The magnetic moment below 100 K is, with 5.7 μ_B, too high for a $S_1 = 0$, $S_2 = 2$ system, but another plausible explanation other than a partial spin transition cannot be found for this behavior. The results from X-ray structure analysis support this theory. The same complex with one additional pyridine in the crystal exhibits a constant magnetic moment around 5 μ_B, typical for a $S_1 = 0$, $S_2 = 2$ system. For $Fe_2$2a × 4Py, two steps around 260 K and 90 K are found. Here also different samples with different steps during the spin transition were obtained depending on the used conditions for the crystallization of the complex, but a whole temperature $S_1 = 0$, $S_2 = 2$ behavior as for $Fe_2$2b × 4Py · Py could not be observed.

Conclusions

The magnetic and structural properties of four new dinuclear iron(II) complexes with pyridine as axial ligands are presented in this paper. With the exception of $Fe_2$2c × 4Py · Py and $Fe_2$2b × 4Py·Py, all complexes perform partial low-spin ⇔ high-spin spin transitions. Results from X-ray structure analysis indicate that the stepwise spin transitions are rather due to a preferred ordering of high-spin ($S_1 = 2$, $S_2 = 2$) and low-spin ($S_1 = 0$, $S_2 = 0$) molecules in the crystal than, as found in the literature for bpym-bridged complexes, due to the formation of a mixed HS-LS species in one molecule. The unusual effective magnetic moment of $Fe_2$2a × 4Py and $Fe_2$2b × 4Py below the transition temperature is than more easily understood, since not necessarily exactly half of the molecules have to perform a spin transition. This spin transition behavior can be equated with a high cooperativeness between the two phenylene-bridged iron centers, which may also be the reason for the small hysteresis observed for the complex $Fe_2$2b × 4Py. For $Fe_2$2a and $Fe_2$2b, a strong dependence of

the SCO behavior on the amount of additional pyridine in the crystal was found and a direct comparison between the samples used for the magnetic measurements and the crystals used for the X-ray structure analysis is therefore not possible.

The pyridine diadducts of the mononuclear complexes of this ligand type also show spin transition behavior for Fe1a and Fe1b. Both crossovers are complete and no steps were observed. The influence of the equatorial ligand on the ligand field strength was found to be (increasing ligand filed strength) **d** < **c** < **b** < **a**. This order cannot be confirmed for the dinuclear complexes. Here the complex $Fe_2$2d with the strongest electron-withdrawing substituents also shows spin transition behavior. Due to the strong influence of additional pyridine in the crystal on the spin state of the complexes, it is difficult to suggest a new order and further experiments are necessary.

ACKNOWLEDGMENTS

The authors thank S. Albrecht for the X-ray measurements, S. Schmidt for the thermo-gravimetric analyses, and G. Nassel for the reproduction of the discussed complexes.

REFERENCES

[1] (a) Gütlich, P.; Hauser, A. Coord Chem Rev 1990, 97, 1–22; (b) Gütlich, P.; Hauser, A.; Spiering, H. Angew Chem Int Ed Engl 1994, 33, 2024; (c) König, E. Structure Bonding 1991, 76, 51–152.

[2] (a) Kahn, O.; Jay Martinez, C. Science 1998, 279, 44–48; (b) Real, J. A.; Gaspar, A. B.; Niel, V.; Munoz, M. C. Coord Chem Rev 2003, 236, 121–141.

[3] (a) Spiering, H.; Kohlhaas, T.; Romstedt, H.; Hauser, A.; Bruns-Yilmaz, C.; Kusz, J.; Gütlich, P. Coord Chem Rev 1999, 190–192, 629–647; (b) Hauser, A.; Jeftic, J.; Romstedt, H.; Hinek, R.; Spiering, H. Coord Chem Rev 1999, 190–192, 471–491.

[4] Niel, V.; Thompson, A. L.; Munoz, M. C.; Galet, A.; Goeta, A. E.; Real, J. A. Angew Chem Int Ed 2003, 42, 3760–3763.

[5] (a) Real, A.; Zarembowitch, J.; Kahn, O.; Solans, X. Inorg Chem. 1987, 26, 2939–2943; (b) Real, J. A.; Castro, I.; Bousseksou, A.; Verdaguer, M.; Burriel, R.; Castro, M.; Linares, J.; Varret, F. Inorg Chem 1991, 36, 455–464; (c) Real, J. A.; Bolvin, H.; Bousseksou, A.; Dworkin, A.; Kahn, O.; Varret, F.; Zarembowitch, J. J Am Chem Soc 1992, 114, 4650–4658; (d) Ksenofontov, V.; Spiering, H.; Reiman, S.; Garcia, Y.; Gaspar, A. B., Moliner, N.; Real, J. A.; Gütlich, P. Chem Phys Lett 2001, 348, 381–386.

[6] Gaspar, A. B.; Ksenofontov, V.; Real, J. A.; Gütlich, P. Chem Phys Lett 2003, 373, 385–391.

[7] (a) Leita, B. A.; Moubaraki. B.; Murray, K. S.; Smith, J. P.; Cashion, J. D. Chem Commun 2004, 156–157; (b) Nakano, K.; Suemura, N.; Kawata, S.; Fuyuhiro, A.; Yagi, T.; Nasu, S.; Morimoto, S.; Kaizaki, S. Dalton Trans 2004, 982–988.

[8] Jäger, E.-G.; Häussler, E.; Rudolph, M.; Schneider, A. Z Anorg Allg Chem 1985, 525, 67–85.

[9] (a) Leibeling, G. Ph.D. Thesis, Universiy of Jena, Germany, 2003; (b) Jäger, E.-G. Chemistry at the Beginning of the Third Millennium; Fabbrizzi, L.; Poggi, A. (Eds:); Springer-Verlag,: Berlin, 2000; pp. 103–138.

[10] Müller, B. R.; Leibeling, G.; Jäger, E.-G. Chem Phys Lett 2000, 319, 368.

[11] Weber, B.; Görls, H.; Jäger, E.-G. Inorg Chem, submitted.

[12] (a) Weber, B.; Görls, H.; Rudolph, M.; Jäger, E.-G. Inorg Chim Acta 2002, 337, 247–265; (b) Weber, B.; Dissertation (Ph.D. Thesis) 2002, Universität Jena, Germany, Der Andere Verlag 2003.

[13] Hasty, E. F.; Colburn, T. J.; Hendrickson, D. N. Inorg Chem 1973, 12, 2414–2421.

[14] Autorenkollektiv: Organikum, Johann Ambrosius Barth Verlagsgesellschaft mbH 1993.

[15] Heyn, B.; Hipler, B.; Kreisel, G.; Schreer, H.; Walter, D. Anorganische Synthesechemie; Springer-Verlag: Heidelberg, 1986; 2. Auflage.

[16] Sheldrick, G. M. Acta Crystallogr Sect A Found Crystallogr 1990, 46, 467–473.

[17] Sheldrick, G. M. SHELXL97; University of Göttingen, Germany, 1993.

[18] Altomare, A.; Burla, M. C.; Camalli, G. M.; Cascarano, G.; Giacovazzo, C.; Guagliardi, A.; Moliterni, A. G. G.; Polidori, G.; Spagna, R. "SIR 97", Campus Universitario Bari, 1997; J Appl Crystallogr 1999, 32, 115–119.

[19] Johnson, C. K.; Burnett, M. N. ORTEP-III; Oak-Ridge National Laboratory, Oak-Ridge 1996; Farrugia, L. J. J Appl Cryst 1997, 30, 565.

[20] CCDC-255643 ($Fe_2$2a × 4Py·4Py), CCDC-255644 ($Fe_2$2b × 4Py·7Py, 200 K), and CCDC-255645 ($Fe_2$2b × 4Py·7Py, 125 K) contains the supplementary crystallographic data for this paper. These data can be obtained free of charge via www.ccdc.cam.ac.uk/conts/retrieving.html (or from the Cambridge Crystallographic Data Centre, 12, Union Road, Cambridge CB2 1EZ, UK; fax: (+44) 1223-336-033; or deposit@ccdc.cam.ac.uk).

[21] Görls, H.; Jäger, E.-G. Cryst Res Technol 1991, 26, 349.